

Evolution of beam distribution in crossing a Walkinshaw resonance

S.Y. Lee¹, K.Y. Ng², H. Liu¹, H.C. Chao¹

¹*Indiana University, Bloomington, IN 47405*

²*Fermilab, Batavia, IL 60510*

Abstract

The third-integer coupling resonance at $\nu_x - 2\nu_z = \ell$, known as the Walkinshaw resonance, is important in high-power accelerators. We find that when the betatron tunes ramp through a Walkinshaw resonance, the fractional emittance growth (FEG) is a universal function of the effective resonance strength: $G_{1,-2,\ell} \sqrt{\epsilon_{xi}} |\Delta(\nu_x - 2\nu_z)/\Delta n|^{-1/2}$, where $G_{1,-2,\ell}$ is the resonance strength, ϵ_{xi} and ϵ_{zi} are the initial horizontal and vertical emittances, respectively, and $|\Delta(\nu_x - 2\nu_z)/\Delta n|$ is the resonance crossing rate per revolution. At large effective resonance strengths, the FEG reaches an asymptotic maximum value $(\text{FEG})_{\text{max}} \sim 2\epsilon_{xi}/\epsilon_{zi}$ for $\epsilon_{xi} \gg \frac{1}{2}\epsilon_{zi}$, or $\epsilon_{zi}/(2\epsilon_{xi})$ for $\epsilon_{xi} \ll \frac{1}{2}\epsilon_{zi}$. There is little emittance exchange at $\epsilon_{xi} = \frac{1}{2}\epsilon_{zi}$, which can be used to minimize emittance growth in crossing a Walkinshaw resonance.

Published in

Phys. Rev. Lett. **110**, 094801 (2013)

Evolution of beam distribution in crossing a Walkinshaw resonance

S.Y. Lee¹, K.Y. Ng², H. Liu¹ and H.C. Chao¹
¹*Department of Physics, IU, Bloomington, IN 47405*
²*Fermilab, P.O. Box 500, Batavia, IL 60510*
 (Dated: January 9, 2013)

The third-integer coupling resonance at $\nu_x - 2\nu_z = \ell$, known as the Walkinshaw resonance, is important in high-power accelerators. We find that when the betatron tunes ramp through a Walkinshaw resonance, the fractional emittance growth (FEG) is a universal function of the effective resonance strength: $G_{1,-2,\ell} \sqrt{\epsilon_{xi}} |\Delta(\nu_x - 2\nu_z)/\Delta n|^{-1/2}$, where $G_{1,-2,\ell}$ is the resonance strength, ϵ_{xi} and ϵ_{zi} are the initial horizontal and vertical emittances, respectively, and $|\Delta(\nu_x - 2\nu_z)/\Delta n|$ is the resonance crossing rate per revolution. At large effective resonance strengths, the FEG reaches an asymptotic maximum value $(\text{FEG})_{\text{max}} \sim 2\epsilon_{xi}/\epsilon_{zi}$ for $\epsilon_{xi} \gg \frac{1}{2}\epsilon_{zi}$, or $\epsilon_{zi}/(2\epsilon_{xi})$ for $\epsilon_{xi} \ll \frac{1}{2}\epsilon_{zi}$. There is little emittance exchange at $\epsilon_{xi} = \frac{1}{2}\epsilon_{zi}$, which can be used to minimize emittance growth in crossing a Walkinshaw resonance.

PACS numbers: 29.20.-c, 29.20.Dh, 41.60.Ap, 41.85.-p

Low-order coupling resonances are of concern to the design and operation of circular accelerators. The third-integer difference resonance $\nu_x - 2\nu_z = \ell$, known as the Walkinshaw resonance, is sometimes unavoidable in many high-power accelerators, such as isochronous cyclotrons, nonscaling FFAGs, and other low-energy accelerators. This resonance becomes a focus of design and operation of all cyclotrons [1]. It has been termed “formidable barrier” and “impassable” [2], and may cause emittance growths and beam loss. Although all the adverse effects of the resonance have long been experienced, however, the dynamic of emittance growths has not been fully analyzed and understood. So far the only means of reducing emittance growths have been fast passage and the reduction of the resonance strength.

There had been theoretical analysis on the $\nu_x - 2\nu_z$ resonance [2, 3], and subsequent experimental measurements in storage rings [4, 5]. These papers, however, deal essentially with single-particle motion near the resonance at fixed betatron tunes. This paper investigates instead the beam dynamics while the betatron tunes ramp through the third-integer coupling resonance. We study emittance growths and scaling laws. Methods are given to alleviate the emittance growth. Hopefully, beam power improvement could become possible.

In term of the horizontal and vertical action-angle coordinates (J_x, ϕ_x) and (J_z, ϕ_z) , the Hamiltonian near the $\nu_x - 2\nu_z = \ell$ resonance can be approximated as [5, 6]

$$H = \nu_x J_x + \nu_z J_z + \frac{1}{2}\alpha_{xx} J_x^2 + \alpha_{xz} J_x J_z + \frac{1}{2}\alpha_{zz} J_z^2 + G_{1,-2,\ell} J_x^{1/2} J_z \cos(\phi_x - 2\phi_z - \ell\theta + \xi_{1,-2,\ell}) + \dots$$

Here, the orbiting angle $\theta = s/R$ serves as the “time coordinate,” R is the mean radius, ν_x and ν_z are respectively the horizontal and vertical betatron tunes, ℓ is an integer, and the nonlinear detuning parameters are

$$\alpha_{xx,zz} = - \oint \frac{\beta_{x,z}^2 B_z'''}{16\pi B\rho} ds, \quad \alpha_{xz} = \oint \frac{\beta_x \beta_z B_z'''}{8\pi B\rho} ds.$$

The resonance strength $G_{1,-2,\ell} \geq 0$ and its phase $\xi_{1,-2,\ell}$ are represented by

$$G_{1,-2,\ell} e^{j\xi_{1,-2,\ell}} = \frac{\sqrt{2}}{8\pi} \oint \beta_x^{1/2} \beta_z \frac{B_z''(s)}{B\rho} \times e^{j[\chi_x(s) - 2\chi_z(s) - (\nu_x - 2\nu_z - \ell)\theta]} ds,$$

where $\beta_{x,y}$ and $\chi_{x,y}(s) = \int_0^s ds'/\beta_{x,y}(s')$ are the horizontal/vertical betatron functions and betatron phases. In above, B_z'' and B_z''' are, respectively, the sextupole and octupole magnetic field components around the ring, with $B\rho$ representing the rigidity of the beam.

The Hamiltonian is canonically transformed to the rotating frame using the generating function:

$$F_2(\phi_x, \phi_z, J_1, J_2) = (\phi_x - 2\phi_z - \ell\theta + \xi_{1,-2,\ell})J_1 + \phi_z J_2.$$

The coordinate transformation is

$$\begin{aligned} \phi_1 &= \phi_x - 2\phi_z - \ell\theta + \xi_{1,-2,\ell}, & J_x &= J_1, \\ \phi_2 &= \phi_z, & J_z &= -2J_1 + J_2, \end{aligned}$$

and the new Hamiltonian becomes $\tilde{H} = H_1(J_1, \phi_1, J_2) + H_2(J_2)$, where $H_2(J_2) = \nu_z J_2 + \frac{1}{2}\alpha_{22} J_2^2$ and

$$H_1(J_1, \phi_1, J_2) = \delta J_1 + \frac{1}{2}\alpha_{11} J_1^2 + \alpha_{12} J_1 J_2 + G_{1,-2,\ell} J_1^{1/2} (J_2 - 2J_1) \cos(\phi_1). \quad (1)$$

Here $\delta = \nu_x - 2\nu_z - \ell$ is the resonance proximity parameter and the transformed detuning parameters are $\alpha_{11} = \alpha_{xx} - 4\alpha_{xz} + 4\alpha_{zz}$, $\alpha_{12} = \alpha_{xz} - 2\alpha_{zz}$, and $\alpha_{22} = 4\alpha_{zz}$. Hamilton's equations of motion are $\frac{dJ_2}{d\theta} = -\frac{\partial \tilde{H}}{\partial \phi_2} = 0$, $\frac{d\phi_2}{d\theta} = \frac{\partial \tilde{H}}{\partial J_2}$, and

$$\frac{dJ_1}{d\theta} = -\frac{\partial \tilde{H}}{\partial \phi_1} = G_{1,-2,\ell} J_1^{1/2} (J_2 - 2J_1) \sin(\phi_1), \quad (2)$$

$$\begin{aligned} \frac{d\phi_1}{d\theta} &= \frac{\partial \tilde{H}}{\partial J_1} = \delta + \alpha_{12} J_2 + \alpha_{11} J_1 \\ &+ G_{1,-2,\ell} \frac{J_2 - 6J_1}{2J_1^{1/2}} \cos(\phi_1). \end{aligned} \quad (3)$$

Particle dynamics obey Eqs. (2) and (3) at constant J_2 and H_1 , which are invariants if the betatron tunes are not changed. However, we study the dynamics of particle motion during the passage of a resonance. The rate of resonance crossing is normally small, and thus H_1 are still quasi-constant of motion for each particle.

The fixed points of the Hamiltonian H_1 are obtained by equating both Eqs. (2) and (3) to zero. Two unstable fixed points (UFP) are located at the intersection between the Courant-Snyder (CS) circle ($2J_1 = J_2$) and the coupling arc. Separatrices at other various conditions have been shown in Ref. [3]. Figure 2 in Ref. [5] shows also experimental data of one of the separatrices for this resonance, where the CS and coupling circles are expressed in phase space coordinates: $(X, P) = (\sqrt{2\beta_x J_1} \cos \phi_1, -\sqrt{2\beta_x J_1} \sin \phi_1)$ with β_x being the horizontal betatron-function at the observation point. The separatrix is the Hamiltonian torus that passes through the UFP; i.e.,

$$\frac{1}{2}(J_2 - 2J_1) \left\{ -\delta - \frac{1}{2}\alpha_{11} \left(J_1 + \frac{J_2}{2} \right) - \alpha_{12} J_2 + 2G_{1,-2,\ell} J_1^{1/2} \cos(\phi_1) \right\} = 0,$$

which is composed of a CS circle $2J_1 = J_2$, and a coupling arc $\alpha_{11}(2J_1) - 4\sqrt{2}G_{1,-2,\ell}\sqrt{2J_1}\cos\phi_1 + 4\delta + 4\alpha_{12}J_2 + \alpha_{11}J_2 = 0$. For particles with $2J_1 < J_2$, their flows revolve around the stable fixed points at $\phi = 0$ or π , and $2\alpha_{11}J_1^{3/2} \mp 6G_{1,-2,\ell}J_1 + 2(\delta + \alpha_{12}J_2)J_1^{1/2} \pm G_{1,-2,\ell}J_2 = 0$. Experimental data depicting the Hamiltonian flow of these particles have been shown in Fig. 7 of Ref. [5].

Now, we study the effects of the Walkinshaw resonance on a beam of particles. When the betatron tunes ramp through a Walkinshaw resonance, all fixed points move across the beam, and the beam distribution will evolve as well. Consider a beam with bi-Gaussian distribution

$$\rho_2(J_x, J_z) = \frac{1}{\epsilon_x \epsilon_z} \exp \left\{ -\frac{J_x}{\epsilon_x} - \frac{J_z}{\epsilon_z} \right\}, \quad (4)$$

where ϵ_x and ϵ_z are, respectively, the horizontal and vertical rms emittances of the beam [6]. Now J_x and J_z are transformed to J_1 and J_2 . The invariant distribution function in J_2 can be obtained by integrating over J_1 :

$$\rho_1(J_2) = \frac{1}{2\epsilon_x - \epsilon_z} \left[\exp \left(-\frac{J_2}{2\epsilon_x} \right) - \exp \left(-\frac{J_2}{\epsilon_z} \right) \right]. \quad (5)$$

As the betatron tunes ramp through the $\nu_x - 2\nu_z = \ell$ resonance, the action J_2 is invariant, and the distribution function $\rho_1(J_2)$ is invariant. The first moment $\langle J_2 \rangle = 2\epsilon_x + \epsilon_z$ is also invariant, and thus $\Delta\epsilon_z = -2\Delta\epsilon_x$. For the above bi-Gaussian distribution, the maximum of the invariant distribution function occurs at

$$J_{2,\max} = \frac{2\epsilon_x \epsilon_z}{2\epsilon_x - \epsilon_z} \ln \frac{2\epsilon_x}{\epsilon_z}.$$

Since J_2 varies from particle to particle, it is advantageous to study the beam distribution in the variable

$u = J_1/J_2$. The transformed beam distribution is

$$\rho_{2a}(u, J_2) = \frac{J_2}{\epsilon_x \epsilon_z} \exp \left\{ -\left(\frac{u}{\epsilon_x} + \frac{1-2u}{\epsilon_z} \right) J_2 \right\}, \quad (6)$$

where the variables $u \in [0, \frac{1}{2}]$ and $J_2 \in [0, \infty]$. In this representation, all particles in the beam have the same CS circle at $u = J_1/J_2 = 1/2$. We also note that when $\epsilon_x = \frac{1}{2}\epsilon_z$, $\rho_{2a}(u, J_2)$ is independent of u for all J_2 . Integrating over J_2 , we find the 1D distribution as

$$\rho_{1a}(u) = \frac{\epsilon_x/\epsilon_z}{[\epsilon_x/\epsilon_z + (1-2\epsilon_x/\epsilon_z)u]^2}, \quad u \in \left[0, \frac{1}{2} \right]. \quad (7)$$

which is plotted in Fig. 1. When $\epsilon_{xi} > \frac{1}{2}\epsilon_{zi}$, there are more particles at higher J_1 actions, and we expect that the horizontal emittance will decrease in crossing a Walkinshaw resonance. Conversely, when $\epsilon_{xi} < \frac{1}{2}\epsilon_{zi}$, the horizontal emittance will increase in crossing the Walkinshaw resonance. At the condition $\epsilon_{xi} = \frac{1}{2}\epsilon_{zi}$, the distribution function is uniform, and we expect no emittance exchange during the crossing of a Walkinshaw resonance.

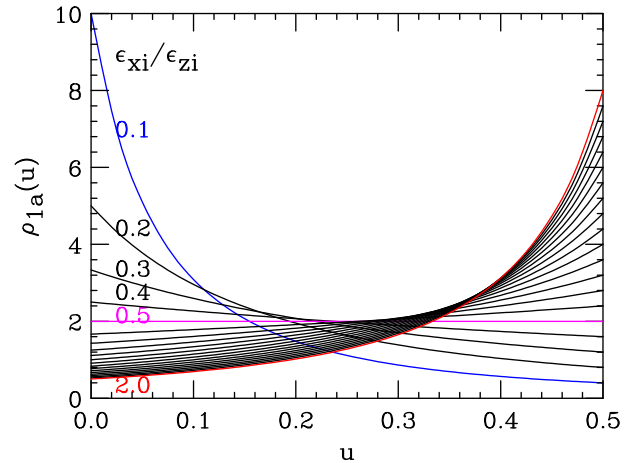


FIG. 1: The distribution of a bi-Gaussian beam in the $u = J_1/J_2$ action coordinate, for various horizontal and vertical emittance ratios, $\epsilon_{xi}/\epsilon_{zi} = 0.1, 0.2, \dots, 2.0$. If $\epsilon_{xi} > \frac{1}{2}\epsilon_{zi}$, there are more particles with higher $J_1 = J_x$ actions, and vice versa. The distribution is uniform when $\epsilon_{xi} = \frac{1}{2}\epsilon_{zi}$.

When the betatron tunes ramp through a $\nu_x - 2\nu_z = \ell$ resonance with $\epsilon_{xi} > \frac{1}{2}\epsilon_{zi}$, there are more particles with higher horizontal actions. They are drawn along the coupling arc towards the center of the CS circle with their actions reduced, thus decreasing the horizontal beam emittance. Since $J_2 = 2J_x + J_z$ is an invariant, their vertical actions will increase and so will the vertical emittance of the beam. This process is nearly independent of the detuning parameters of the accelerator. Noting that $2\Delta\epsilon_x + \Delta\epsilon_z$, we define the *fractional emittance growth* (FEG) of a difference resonance as

$$\begin{aligned} \text{FEG} &\equiv \left| \frac{\Delta\epsilon_x}{\epsilon_{xi}} \right| + \left| \frac{\Delta\epsilon_z}{\epsilon_{zi}} \right| \\ &= \left| \frac{\Delta\epsilon_x}{\epsilon_{xi}} \right| \left(\frac{2\epsilon_{xi}}{\epsilon_{zi}} + 1 \right) = \left| \frac{\Delta\epsilon_z}{\epsilon_{zi}} \right| \left(\frac{\epsilon_{zi}}{2\epsilon_{xi}} + 1 \right). \quad (8) \end{aligned}$$

The definition of the FEG is not unique. One may define it as $|\Delta\epsilon_x/\epsilon_{xi}|$, or $\Delta\epsilon_z/\epsilon_{zi}$ or simply $\Delta\epsilon_x/\epsilon_{xi} + \Delta\epsilon_z/\epsilon_{zi}$. These other definitions can not provide full range of scaling properties that we will discuss in the text below.

Multi-particle simulations were performed to study the dynamics of resonance crossing. Details of these simulations have been published in Ref. [7]. Macro-particles, typically 5000, are populated in bi-Gaussian distribution with initial rms emittances ϵ_{xi} and ϵ_{zi} . The rms beam emittances are computed by using the second moments of the phase-space distributions [6] at each revolution. Sextupoles are used to control the strength of the Walkinshaw resonance, and octupoles are used to control the detuning parameters. The betatron tunes are varied linearly to cross a $\nu_x - 2\nu_z = \ell$ resonance. Figure 2 shows the evolution of the horizontal and vertical emittances during the crossing the difference resonance with α_{11} rang-

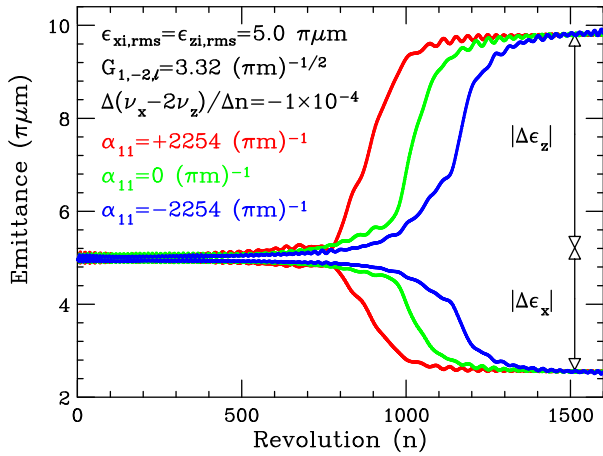


FIG. 2: The resonance crossing rate is -1.0×10^{-4} for a third-integer difference resonance with resonance strength $G_{1,-2,\ell} = 3.328 (\pi\text{m})^{-1/2}$ and $\epsilon_{xi} = \epsilon_{zi} = 5.0 \pi\mu\text{m}$. The detuning parameters are $\alpha_{11} = 0$ and $\pm 2254 (\pi\text{m})^{-1}$.

ing from -2254 to $+2254 (\pi\text{m})^{-1}$, which correspond to a tune spread of $6\alpha_{11}\epsilon_{xi} \approx 0.067$ within the beam. Although the beam emittances evolve faster or slower across the resonance according to the detuning parameters due to crossing the resonance earlier or later, the final FEGs are independent of the detuning parameters. Simulations with larger emittances will reach the same conclusions as will be demonstrated later. In FFAG accelerators and cyclotrons, the ramp rates depend on the available rf systems. One would try to ramp through the resonances as fast as possible to avoid adverse effects. The typical tune-ramp rate is about $10^{-3} \sim 10^{-5}$ per revolution, and we use these typical tune-ramp rate for our simulations. At these tune ramp rates, the beam particles follow their Hamiltonian flow, one can say that their motion is adiabatic. Particle motion in accelerator usually obeys the adiabatic condition in resonance crossing.

Now, we study the scaling properties of the FEG vs accelerator parameters. Figure 3 shows results of

simulations with $\epsilon_{xi} = \epsilon_{zi}$. The FEGs depend essen-

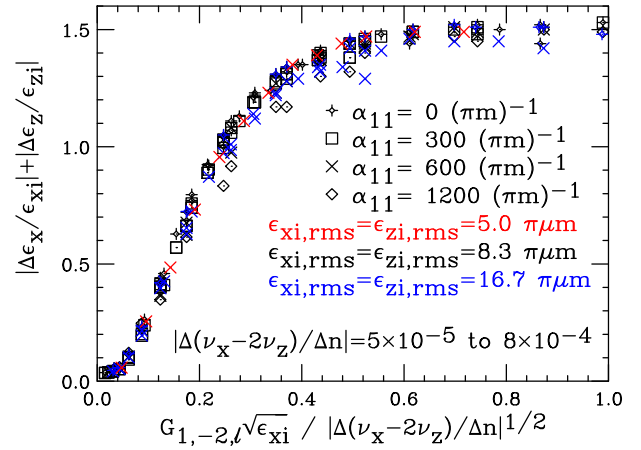


FIG. 3: The FEG vs the effective resonance parameter for initially equal-emittance-Gaussian-distributed beams. Note that the FEG depends only on a single effective resonance strength: $G_{1,-2,\ell}\sqrt{\epsilon_{xi}}/\sqrt{|\Delta(\nu_x - 2\nu_z)/\Delta n|}$. The FEGs are independent of the detuning parameters α_{11} .

tially on a single effective resonance strength parameter $G_{\text{eff}} = G_{1,-2,\ell}\sqrt{\epsilon_{xi}}/\sqrt{|\Delta(\nu_x - 2\nu_z)/\Delta n|}$, but are independent of detuning parameters. Note that the maximum FEG for equal initial emittances is about 1.5. This means that the maximum fractional emittance growth in the vertical plane is about 1.0, and the maximum fractional horizontal emittance reduction is about 0.5.

Figure 1 shows that there are more particles in lower J_1 actions when $\epsilon_{xi} < \frac{1}{2}\epsilon_{zi}$. Thus the horizontal emittance will increase and the vertical emittance will decrease. Figure 4 shows the emittance exchange for $\epsilon_{xi} = 1 \pi\mu\text{m}$, and $\epsilon_{zi} = 10 \pi\mu\text{m}$ with $|\Delta(\nu_x - 2\nu_z)/\Delta n| = 8 \times 10^{-5}$. The horizontal emittance increases while the vertical emittance decreases with the FEG ~ 4.5 .

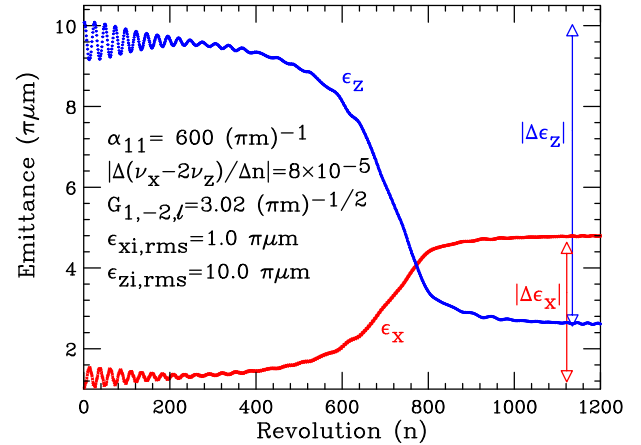


FIG. 4: The resonance crossing rate is -8.0×10^{-5} for a third-integer difference resonance of strength $G_{1,-2,\ell} = 3.02 (\pi\text{m})^{-1/2}$ and $\epsilon_{xi} = 1.0 \pi\mu\text{m}$, and $\epsilon_{zi} = 10.0 \pi\mu\text{m}$. The detuning parameter is fixed at $\alpha_{11} = 600 (\pi\text{m})^{-1}$.

According to the FEG scaling law in Eq. (8), when

$2\epsilon_{xi} \gg \epsilon_{zi}$, the maximum FEG is $\sim 2\epsilon_{xi}/\epsilon_{zi}$, and when $2\epsilon_{xi} \ll \epsilon_{zi}$, the maximum FEG is $\sim \epsilon_{zi}/(2\epsilon_{xi})$. Figure 5 gathers a large amount of simulation data, depicting the FEG vs $\epsilon_{xi}/\epsilon_{zi}$. The dashed and dotted lines show the asymptotic maxima FEG = $2\epsilon_{xi}/\epsilon_{zi}$ and $\epsilon_{zi}/(2\epsilon_{xi})$ of Eq. (8). At $\epsilon_{xi} \approx \frac{1}{2}\epsilon_{zi}$, there is little emittance exchange. Although Fig. 1 is based on bi-Gaussian distribution, the FEG scaling law works for other distributions as well. The circle, rectangular and diamond symbols in Fig. 5 represent the results for a beam with an initial uniform beam distribution in both or one of the horizontal and vertical phase spaces. If the initial beam distribution in the horizontal and vertical planes are independent, and has the same functional form, i.e., $\rho_3(J_x, J_z) = f(J_x/\epsilon_x)f(J_z/\epsilon_z)$, the corresponding beam distribution function $\rho_{3a}(u, J_2)$ will be symmetric in the u -variable about $\epsilon_x = \frac{1}{2}\epsilon_z$. Thus there will be no net emittance exchange because there are equal number of particles that increase or decrease their actions in crossing the resonance.

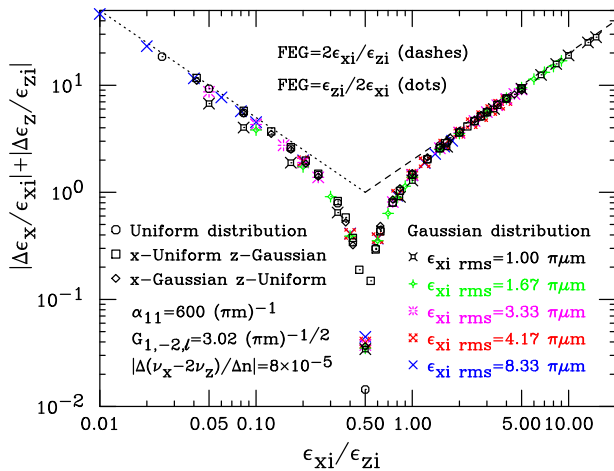


FIG. 5: The maximum fractional emittance growth (FEG) vs $\epsilon_{xi}/\epsilon_{zi}$. The dashed and dotted lines correspond to $FEG_{\max} \approx 2\epsilon_{xi}/\epsilon_{zi}$ and $\epsilon_{zi}/2\epsilon_{xi}$. Note that near $\epsilon_{xi} \sim 0.5\epsilon_{zi}$, there is no emittance exchange. The circle symbols correspond to uniform distribution in both transverse phase spaces, and all other data are obtained from bi-Gaussian distribution.

In conclusion, multi-particle simulations and Hamiltonian dynamics are employed to study beam property in crossing a Walkinshaw resonance. We find that the emittance growth obeys a scaling law depending essentially on a dimensionless effective resonance strength parameter: $G_{1,-2,\ell}\sqrt{\epsilon_{xi}}|\Delta(\nu_x - 2\nu_z)/\Delta n|^{-1/2}$ (see Fig. 3), which is detuning independent. The fractional emittance growth (FEG) reaches a maximum saturation value at a large effective resonance strength. The maximum FEG depends essentially on $\epsilon_{xi}/\epsilon_{zi}$. For $2\epsilon_{xi} \gg \epsilon_{zi}$, the maximum FEG $\sim 2\epsilon_{xi}/\epsilon_{zi}$, and for $2\epsilon_{xi} \ll \epsilon_{zi}$, the maximum FEG is $\epsilon_{zi}/(2\epsilon_{xi})$ as shown in Fig. 5. If the initial emittances of the beam are known, one can predict the emittances after crossing a strong third-integer coupling resonance.

To avoid emittance exchange in passing through a Walkinshaw resonance, we can prepare a beam with an initial horizontal emittance equal to half of the vertical. The minimization of emittance growths and beam loss crossing a Walkinshaw resonance could hopefully lead to an improvement in beam currents in circular accelerators.

Now we consider a beam with equal initial horizontal and vertical emittance ϵ_0 . After passing through a strong $\nu_x - 2\nu_z$ resonance, the final emittances will be $\epsilon_x \approx \frac{1}{2}\epsilon_0$ and $\epsilon_z \approx 2\epsilon_0$. If the vertical aperture is not an issue, the smaller horizontal emittance can pass through a smaller magnetic/electric septum gap. If this resulting beam is made to pass through the same resonance again at a similarly strong strength, the horizontal emittance and vertical emittance will be exchanged again and restored to its original values; i.e., the final beam emittances are $\epsilon_x \approx \epsilon_z \approx \epsilon_0$. All these predictions can be tested experimentally in a cyclotron or circular accelerators.

Acknowledgments

This work is supported in part by grants from the US DOE, under contract DE-FG0292ER40747, DE-AC-02-76CH030000, and the National Science Foundation NSF PHY-1205431. We thank many useful comments from M. Craddock and R. Baartman.

- [1] S. Turner, ed. *Cyclotrons, Linacs and their applications*, CERN 96-02, 1996.
- [2] A.A. Garren, D.L. Judd, L. Smith and H.A. Willax, Nucl. Instru. Meth., **18-19**, 525 (1962).
- [3] Keith Symon, *Applied Hamiltonian Dynamics*, in AIP Conference Proceedings 149, p. 370 ed. M. Month and M. Dienes (AIP, New York, 1992); Keith Symon, ANL report LS-132 (November 1988), unpublished.
- [4] J. Liu, E. Crosbie, L. Teng, J. Bridges, D. Ciarlette, K. Symon, and W. Trzeciak, Part. Accel., **41**, 1 (1993).
- [5] M. Ellison, M. Bali, B. Brabson, J. Budnick, D.D. Caussyn, A.W. Chao, V. Derenchuk, S. Dutt, G. East,

- D. Friesel, B. Hamilton, H. Huang, W.P. Jones, S.Y. Lee, D. Li, M.G. Minty, K.Y. Ng, X. Pei, A. Riabko, T. Sloan, M. Syphers, Y. Wang, Y. Yan, and P.L. Zhang, Phys. Rev. E **50**, 4051 (1994).
- [6] S.Y. Lee, *Accelerator Physics*, 3rd. Ed. (World Scientific Pub., Singapore, 2011).
- [7] S.Y. Lee, Phys. Rev. Lett. **97**, 104801 (2006); S.Y. Lee, G. Franchetti, I. Hofmann, F. Wang, and L. Yang, New J. Phys. **8**, 291 (2006); S.Y. Lee, K.Y. Ng, X. Pang, Y. Jing, and T. Luo, Proceedings of HB2012, Beijing, September 17–21, 2012.